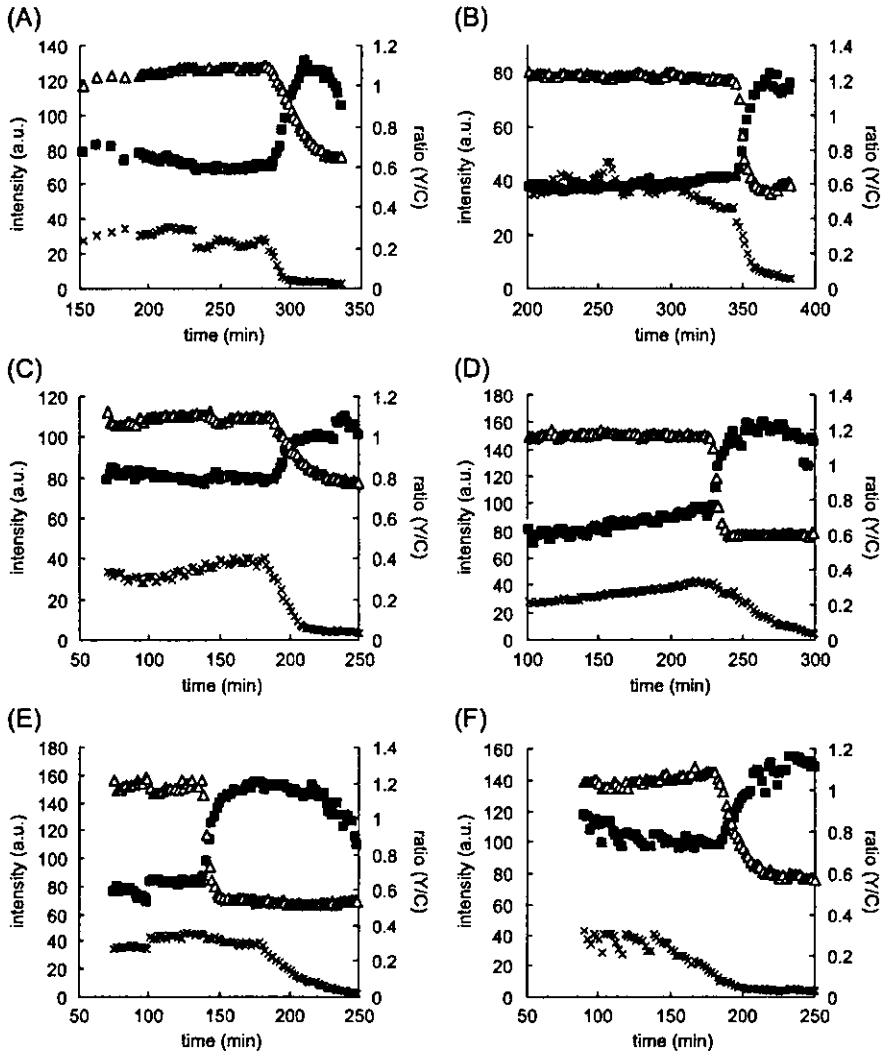

Fig. 6. Fluorescent changes during cell death. HeLa cells expressing the IC-sensor (A, C) or EC-sensor (B, D, E, F) were incubated with 200 ng/ml of TNF-α (A, B) or 3 μM of staurosporine (C, D, E, F). Fluorescent images as shown in Fig. 5 were obtained from each experiment, and then the YFP/CFP ratio and the fluorescence of CFP, YFP, and TMRM for the whole single cell area were quantified and plotted. A–D each show a representative example of each treatment. Filled square (cyan): CFP; filled diamond (yellow): YFP; open triangle: ratio (YFP/CFP); ×: TMRM (red). The vertical axes show the mean pixel intensity of the whole cell region (left; CFP, YFP, and TMRM) and the mean pixel emission ratio of the whole cell region (right; YFP/CFP ratio). a.u., arbitrary units.

activated and the mitochondrial membrane potential reduced, just as in the TNF-α-treated cells (Fig. 5). The temporal relationship between the caspase activation and the morphological changes probably differs in these two treatments. We speculated that other factor(s) are necessary for the morphological changes during cell death to occur, and that these factors are activated almost simultaneously with the caspase in TNF-α-treated cells, whereas it takes time to activate them after the caspase activation in staurosporine-treated cells.

3.6. Temporal relationship of caspase activation and mitochondrial depolarization

Fig. 6(A)–(D) shows typical examples of the fluorescent changes that occurred in each treatment. The fluorescent intensity of the caspase-sensor and TMRM, and the ratio of the YFP and CFP fluorescence of the caspase-sensor were plotted. The horizontal axes indicate the time after the cell death-inducer treatment. Each graph shows the results from a respective single cell. (A) and (C) show the results from cell #1 in Fig. 5(a) and (b), respectively. The emission ratio of YFP/CFP was dramatically reduced, indicating that the caspase was activated at this point in that cell. The fluorescence intensity of TMRM was reduced, indicating that the mitochondria depolarized at this point in that cell. Fig. 6(E) and (F) shows examples with a large time difference between the caspase activation and the mitochondrial depolarization. Caspase activation was observed 44 min earlier than the mitochondrial depolarization in the cell shown in Fig. 6(E), whereas caspase activation was observed 42 min

later than the mitochondrial depolarization in the cell shown in Fig. 6(F).

The YFP emission should have decreased with the caspase activation in ideal FRET system. However, the YFP emission remained constant or increased in some cases (Fig. 6). We considered this to have occurred because the cells shrank immediately after caspase activation, especially in the TNF-α-induced cell death, as shown in Fig. 5. This caused the concentration of the fluorescent protein in the cell, resulting in an increase of the CFP and YFP signals in the confocal slice. This concentration effect was cancelled out by ratiometric analysis. YFP showed unexpected fluorescent changes in some cases, but we were able to evaluate the FRET change properly by analyzing the fluorescent ratio of YFP and CFP.

Sensor proteins were transiently transfected, and the concentration of the sensor proteins was shown to be different in each cell. Some cells expressed a high level of sensor proteins and showed bright fluorescence, and other cells expressed a low level of sensor proteins and showed dim fluorescence. However, we found that the expression level of the sensor proteins did not affect the slope of the ratio trace.

In order to study the temporal relationship between the caspase activation and the mitochondrial depolarization, we carried out a quantitative analysis and estimated the relative timing of the initiator- and effector-caspase activation and mitochondrial depolarization. The starting point of the reduction of the YFP/CFP ratio (A, indicated by an arrow in Fig. 7(a)) and that of the TMRM fluorescence (B, indicated by an arrowhead in Fig. 7(a)) were determined as the time point after which the value decreased during four continuous points or more, the value decreased more than 20% in total, and the reduction of the value was the last one in the experiment. We determined these points in each cell, and calculated the time interval from B to A. We analyzed 31–47 cells in at least seven independent experiments for each treatment, and plotted the results in Fig. 7(b). Here, each plot represents the result from a cell, with time 0 being the point at which the TMRM fluorescence started to decrease. If the plot is on −10, for example, this means that the caspase activation occurred 10 min earlier than the mitochondrial depolarization in that cell. This analysis clarified the temporal relationship between mitochondrial depolarization, initiator caspase activation, and effector caspase activation.

Although Fig. 7 shows some scatter, which suggest that the relationship between caspase activation and mitochondrial depolarization is not firm, we can estimate the relationship between the two by quantitative analysis. A trend was seen in which the median values and mean values of the time interval were estimated to be nearly 0 in all treatments. This means that the caspase activation and mitochondrial depolarization are likely to start within a short amount of time in the majority of cells, compared with the duration from drug treatment to these events, which takes anywhere

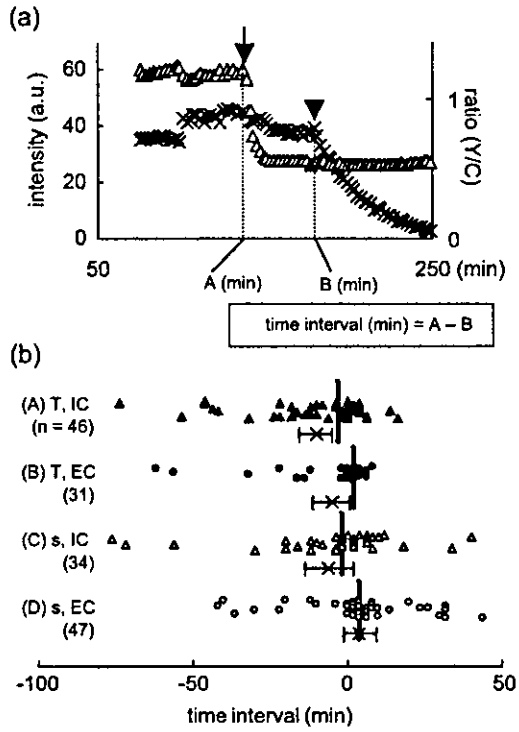

Fig. 7. The time intervals between mitochondrial depolarization and caspase activation. (a) We defined the difference between the two time points indicated by the arrow and arrowhead as the time interval. Details are described in the text. (b) We calculated and plotted this parameter for each cell. Each plot represents one cell. The vertical lines, crosses, and bars represent the median, mean, and 95% confidence interval for each group. The number of cells used in each analysis is shown in parenthesis. Filled mark (A, B): TNF-α; open mark (C, D): staurosporine; triangle (A, C): IC-sensor; circle (B, D): EC-sensor.

from 1 to over 10 h. Because initiator caspases are proteases that cleave and activate effector caspases, the initiator caspase might be activated earlier than the effector caspase. Our results suggest that the effector caspase activation occurred immediately after the initiator caspase activation.

4. Discussion

In this study, we described a method for measuring changes in the initiator or effector caspase activity and mitochondrial membrane potential simultaneously in single living cells in real time by means of bioimaging, which revealed the kinetics of the caspase activation and the relationship among the caspase activities, mitochondrial membrane potential, and morphological changes during cell death. The time schedule of cell death is different in each cell, but dying cells show caspase activation and a reduction of the mitochondrial membrane potential. In a dying cell, it takes a long time, 1–10 h or more, from the addition of cell death-inducers to start initiator caspase activation, and it takes a relatively short time from the initiator caspase activation to start effector caspase activation. This finding

suggests that the caspase cascade proceeds within a short amount of time at the last stage in the entire biochemical process leading to cell death.

Luo et al. [34] reported that the activation of caspase-8 occurred much earlier than that of caspase-3 in TNF-α-induced apoptosis. They calculated the time difference between these activations as about 120 min on average, which differed from ours. They measured the timing of the caspase activation by comparing it with the timing of the morphological change, which is very difficult to determine. In our experiments, we compared the timing of the caspase activation with that of mitochondrial depolarization, which is much easier to analyze objectively, especially in the case of staurosporine-induced cell death, which showed little morphological change (Fig. 5). Therefore, we feel that our conclusion is more reliable.

It is widely accepted that TNF-α brings about cell death via binding with its receptor, receptor trimerization, binding of the intracellular domain of the receptor with adaptor proteins, cleavage (activation) of the initiator caspase (caspase-8), and cleavage (activation) of the effector caspase (caspase-3) [1]. In this study, we investigated the time course of this pathway, and revealed that it takes a long time after drug treatment, more than 10 h in some cases, to start caspase activation. We speculate that this is a period in which initiator caspase activation is prepared for. There are likely some unknown factors which are essential to activating the initiator caspases. These factors delay the cell death process and they determine the timing of cell death. Once these events occur, the activation of caspases and further cell death processes may proceed immediately.

The wide distribution of the plots in Fig. 7 suggests that caspase activation and mitochondrial depolarization are not firmly linked. Some cells showed mitochondrial depolarization earlier than caspase activation, and the other cells showed mitochondrial depolarization later than caspase activation, suggesting that these two events are independently induced in cell death machinery. When cell death is induced via mitochondrial change, cyt. *c* is released from the mitochondria to the cytosol, which is a critical event for cell death [1,8,9]. Cyt. *c* release leads caspase activation by the formation of apoptosome in the cytosol. Both caspase activation and mitochondrial depolarization relate to mitochondrial change, so these reactions occur within a short amount of time in the majority of cells. But these reactions occur with a large time interval in some cells because their relationship is indirect and not rigid. The time schedule of the process leading to each event may respectively depend on individual cellular conditions. Luetjens et al. [40] have reported on the mode of cyt. *c* release, and showed that cyt. *c* was released within 10 min in the majority of cells, whereas cyt. *c* was released stepwise with an intermediate plateau about 30 min in duration in 13% of the release events they observed. In some cells, a certain amount of cyt. *c* was released from the mitochondria to cytosol, which was enough to cause the apoptosome formation and the following caspase activation, but not enough to cause the mitochondrial depolarization because the cyt. *c* remaining in the mitochondria can maintain the membrane potential. Early caspase activation and late mitochondrial depolarization would be observed in this case.

Cyt. *c* release and mitochondrial depolarization have been analyzed using GFP-tagged cyt. *c* and potentiometric dye such as TMRM [41]. It is likely that mitochondrial depolarization is not required and is not sufficient for cyt. *c* release [42], but the temporal relationship between cyt. *c* release and depolarization is still controversial. Some researchers have showed that cyt. *c* was released a long time before mitochondrial depolarization [43,44], whereas others have reported that cyt. *c* release followed mitochondrial depolarization [45]. The timing of mitochondrial depolarization seems to depend on various factors, including the cell death stimulant, cell type, and individual cell condition. The relationship between caspase activation and mitochondrial changes (cyt. *c* release, depolarization) needs to be studied further.

Acknowledgements

This study was supported in part by a grant-in-aid for the Research on Health Sciences focusing on Drug Innovation from the Japan Health Science Foundation, a grant-in-aid for the Research on Advanced Medical Technology from Ministry of Health Labour and Welfare, a grant (MF-16) from the Organization for Pharmaceutical Safety and Research.

References

[1] N.A. Thornberry, Y. Lazebnik, Caspases: enemies within, Science 281 (1998) 1312–1316.
[2] H.R. Stennicke, G.S. Salvesen, Properties of caspases, Biochim. Biophys. Acta 1387 (1998) 17–31.
[3] M.P. Boldin, T.M. Goncharov, Y.V. Goltsev, D. Wallach, Involvement of MACH, a novel MORT1/FADD-interacting protease, in Fas/APO-1- and TNF receptor-induced cell death, Cell 85 (1996) 803–815.
[4] M. Muzio, A.M. Chinnaiyan, F.C. Kischkell, K. O'Rourke, A. Shevchenko, J. Ni, C. Scaffidi, J.D. Bretz, M. Zhang, R. Gentz, M. Mann, P.H. Krammer, M.E. Peter, V.M. Dixit, FLICE, a novel FADD-homologous ICE/CED-3-like protease, is recruited to the CD95 (Fas/APO-1) death-inducing signal complex, Cell 85 (1996) 817–827.
[5] J.P. Medema, C. Scaffidi, F.C. Kischkel, A. Shevchenko, M. Mann, P.H. Krammer, M.E. Peter, FLICE is activated by association with the CD95 death-inducing signaling complex (DISC), EMBO J. 16 (1997) 2794–2804.
[6] D.A. Martin, R.M. Siegel, L. Zheng, M.J. Lenardo, Membrane oligomerization and cleavage activates the caspase-8 (FLICE/MACHα1) death signal, J. Biol. Chem. 273 (1998) 4345–4349.
[7] S.M. Srinivasula, M. Ahmad, T. Fernandes-Alnemri, G. Litwack, E.S. Alnemri, Molecular ordering of the Fas-apoptotic pathway: the Fas/APO-1 protease Mch5 is a CrmA-inhibitable protease that activates multiple Ced-3/ICE-like cysteine proteases, Proc. Natl. Acad. Sci. U. S. A. 93 (1996) 14486–14491.

[8] A. Saleh, S.M. Srinivasula, S. Acharya, R. Fishel, E.S. Alnemri, Cytochrome *c* and dATP-mediated oligomerization of Apaf-1 is a prerequisite for procaspase-9 activation, J. Biol. Chem. 274 (1999) 17941–17945.
[9] E.N. Shiozaki, J. Chai, Y. Shi, Oligomerization and activation of caspase-9, induced by Apaf-1 CARD, Proc. Natl. Acad. Sci. U. S. A. 99 (2002) 4197–4202.
[10] K. Orth, K. O'Rourke, G.S. Salvesen, V.M. Dixit, Molecular ordering of apoptotic mammalian CED-3/ICE-like proteases, J. Biol. Chem. 271 (1996) 20977–20980.
[11] M. Tewari, L.T. Quan, K. O'Rourke, S. Desnoyers, Z. Zeng, D.R. Beidler, G.G. Poirier, G.S. Salvesen, V.M. Dixit, Yama/CPP32β, a mammalian homolog of CED-3, is a CrmA-inhibitable protease that cleaves the death substrate poly(ADP-ribose) polymerase, Cell 81 (1995) 801–809.
[12] A. Ashkenazi, V.M. Dixit, Death receptors: signaling and modulation, Science 281 (1998) 1305–1308.
[13] D.R. Green, J.C. Reed, Mitochondria and apoptosis, Science 281 (1998) 1309–1312.
[14] R.Y. Tsien, The green fluorescent protein, Annu. Rev. Biochem. 67 (1998) 509–544.
[15] A. Miyawaki, J. Llopis, R. Heim, J.M. Mccaffery, J.A. Adams, M. Ikura, R.Y. Tsien, Fluorescent indicators for Ca^{2+} based on green fluorescent proteins and calmodulin, Nature 388 (1997) 882–887.
[16] K. Hirose, S. Kadowaki, M. Tanabe, H. Takeshima, M. Iino, Spatiotemporal dynamics of inositol 1,4,5-trisphosphate that underlies complex Ca^{2+} mobilization patterns, Science 284 (1999) 1527–1530.
[17] M. Zaccolo, F.D. Giorgi, C.Y. Cho, L. Feng, T. Knapp, P.A. Negulescu, S.S. Taylor, R.Y. Tsien, T. Pozzan, A genetically encoded, fluorescent indicator for cyclic AMP in living cells, Nat. Cell Biol. 2 (2000) 25–29.
[18] Y. Nagai, M. Miyazaki, R. Aoki, T. Zama, S. Inouye, K. Hirose, M. Iino, M. Hagiwara, A fluorescent indicator for visualizing cAMP-induced phosphorylation in vivo, Nat. Biotech. 18 (2000) 313–316.
[19] N.P. Dantuma, K. Lindsten, R. Glas, M. Jellne, M.G. Masucci, Short-lived green fluorescent proteins for quantifying ubiquitin/proteasome-dependent proteolysis in living cells, Nat. Biotechnol. 18 (2000) 538–543.
[20] M. Sato, N. Hida, T. Ozawa, Y. Umezawa, Fluorescent indicators for cyclic GMP based on cyclic GMP-dependent protein kinase Iα and green fluorescent proteins, Anal. Chem. 72 (2000) 5918–5924.
[21] T. Nagai, A. Sawano, E.S. Park, A. Miyawaki, Circularly permuted green fluorescent proteins engineered to sense Ca^{2+}, Proc. Natl. Acad. Sci. U. S. A. 98 (2001) 3197–3202.
[22] K. Kurokawa, N. Mochizuki, Y. Ohba, H. Mizuno, A. Miyawaki, M. Matsuda, A pair of fluorescent resonance energy transfer-based probes for tyrosine phosphorylation of the CrkII adaptor protein in vivo, J. Biol. Chem. 276 (2001) 31305–31310.
[23] J. Zhang, Y. Ma, S.S. Taylor, R.Y. Tsien, Genetically encoded reporters of proein kinase A activity reveal impact of substrate tethering, Proc. Natl. Acad. Sci. U. S. A. 98 (2001) 14997–15002.
[24] A.Y. Ting, K.H. Kain, R.L. Klemke, R.Y. Tsien, Geneically encoded fluorescent reporters of protein kinase activities in living cells, Proc. Natl. Acad. Sci. U. S. A. 98 (2001) 15003–15008.
[25] M. Sato, T. Ozawa, K. Inukai, T. Asano, Y. Umezawa, Fluorescent indicators for imaging protein phosphorylation in single living cells, Nat. Biotechnol. 20 (2002) 287–294.
[26] J.D. Violin, J. Zhang, R.Y. Tsien, A.C. Newton, A genetically encoded fluorescent reporter reveals oscillatory phosphorylation by protein kinase C, J. Cell Biol. 161 (2003) 899–909.
[27] K. Truong, M. Ikura, The use of FRET imaging microscopy to detect protein–protein interactions and protein conformational changes in vivo, Curr. Opin. Struck. Biol. 11 (2001) 573–578.
[28] L. Tyas, V.A. Brophy, A. Pope, A.J. Rivett, J.M. Tavaré, Rapid caspase-3 activation during apoptosis revealed using fluorescence-resonance energy transfer, EMBO Rep. 1 (2000) 266–270.
[29] M. Rehm, H. Düßmann, R.U. Jänicke, J.M. Tavaré, D. Kögel, J.H.M. Prehn, Single-cell fluorescence resonance energy transfer analysis demonstrates that caspase activation during apoptosis is a rapid process: role of caspase-3, J. Biol. Chem. 277 2002, pp. 24506–24514.
[30] K.Q. Luo, V.C. Yu, Y. Pu, D.C. Chang, Application of the fluorescence resonance energy transfer method for studying the dynamics of caspase-3 activation during UV-induced apoptosis in living HeLa cells, Biochem. Biophys. Res. Commun. 283 (2001) 1054–1060.
[31] M.J. Morgan, A. Thorburn, Measurement of caspase activity in individual cells reveals differences in the kinetics of caspase activation between cells, Cell Death Differ. 8 (2001) 38–43.
[32] R. Ohnuki, A. Nagasaki, H. Kawasaki, T. Baba, T.Q.P. Uyeda, K. Taira, Confirmation by FRET in individual living cells of the absence of significant amyloid β-mediated caspase 8 activation, Proc. Natl. Acad. Sci. U. S. A. 99 (2002) 14716–14721.
[33] K. Takemoto, T. Nagai, A. Miyawaki, M. Miura, Spatio-temporal activation of caspase revealed by indicator that is insensitive to environmental effects, J. Cell Biol. 160 (2003) 235–243.
[34] K.Q. Luo, V.C. Yu, Y. Pu, D.C. Chang, Measuring dynamics of caspase-8 activation in a single living HeLa cell during TNFalpha-induced apoptosis, Biochem. Biophys. Res. Commun. 304 (2003) 217–222.
[35] T. Fernandes-Alnemri, G. Litwack, E.S. Alnemri, CPP32, a novel human apoptotic protein with homology to *Caenorhabditis elegans* cell death protein Ced-3 and mammalian interleukin-1 beta-converting enzyme, J. Biol. Chem. 269 (1994) 30761–30764.
[36] H. Suzuki, K. Uchida, H. Shima, T. Sato, T. Okamoto, T. Kimura, M. Miwa, Molecular cloning of cDNA for human poly(ADP-rybose) polymerase and expression of its gene during HL-60 cell differentiation, Biochem. Biophys. Res. Commun. 146 (1987) 403–409.
[37] R.C. Scaduto Jr., L.W. Grotyohann, Measurement of mitochondrial membrane potential using fluorescent rhodamine derivatives, Biophys. J. 76 (1999) 469–477.
[38] C.J. Donahue, M. Santoro, D. Hupe, J.M. Jones, B. Pollok, R. Heim, D. Giegel, Correlating cell cycle with apoptosis in a cell line expressing a tandem green fluorescent protein substrate specific for group II caspases, Cytometry 45 (2001) 225–234.
[39] F. Yamasaki, S. Hama, H. Yoshioka, Y. Kajiwara, K. Yahara, K. Sugiyama, Y. Heike, K. Arita, K. Kurisu, Staurosporine-induced apoptosis is independent of p16 and p21 and achieved via arrest at G2/M and at G1 in U251MG human glioma cell line, Cancer Chemother. Pharmacol. 51 (2003) 271–283.
[40] C.M. Luetjens, D. Kögel, C. Reimertz, H. Dübmann, A. Renz, K. Schulze-Osthoff, A.-L. Nieminen, M. Poppe, J.H.M. Prehn, Multiple kinetics of mitochondrial cytochrome *c* release in drug-induced apoptosis, Mol. Pharmacol. 60 (2001) 1008–1019.
[41] H. Düssmann, D. Kögel, M. Rehm, J.H.M. Prehn, Mitochondrial membrane permeabilization and superoxide production during apoptosis: a single-cell analysis, J. Biol. Chem. 278 (2003) 12645–12649.
[42] M.L.R. Lim, M.-G. Lum, T.M. Hansen, X. Roucou, P. Nagley, On the release of cytochrome *c* from mitochondria during cell death signaling, J. Biomed. Sci. 9 (2002) 488–506.
[43] J.C. Goldstein, N.J. Waterhouse, P. Juin, G.I. Evan, D.R. Green, The coordinate release of cytochrome *c* during apoptosis is rapid, complete and kinetically invariant, Nat. Cell Biol. 2 (2000) 156–162.
[44] M. Madesh, B. Antonsson, S.M. Srinivasula, E.S. Alenemri, G. Hajnóczky, Rapid kinetics of tBid-induced cytochrome *c* and Smac/DIABLO release and mitochondrial depolarization, J. Biol. Chem. 277 (2002) 5651–5659.
[45] F. De Giorgi, L. Lartigue, M.K.A. Baure, A. Schubert, S. Grimm, G.T. Hanson, S.J. Remington, R.J. Youle, F. Ichas, The permeability transition pore signals apoptosis by directing Bax translocation and multimerization, FASEB J. 16 (2002) 607–609.

Original Paper

Pharmacology

Pharmacology 2004;72:51–56
DOI: 10.1159/000078632

Received: August 21, 2003
Accepted after revision: February 12, 2004

Itch-Scratch Responses Induced by Lysophosphatidic Acid in Mice

Terumasa Hashimoto Hisayuki Ohata Kazutaka Momose

Department of Pharmacology, School of Pharmaceutical Sciences, Showa University, Tokyo, Japan

Key Words

Lysophosphatidic acid · Rho-associated protein kinase · Itch-scratch response · Histamine · Capsaicin · Mice, lysophosphatidic acid induced itch-scratch response

Abstract

The present investigation was conducted in order to determine whether lysophosphatidic acid (LPA) induces itch-scratch responses (ISRs) in mice. Intradermal administration of LPA induces ISRs; furthermore, the time course for LPA-induced ISRs was similar to that for histamine-induced responses. Comparative study of the pruritogenic activity revealed that histamine possessed a potent effect characterized by a dose-response relationship; however, prostaglandin D_2 failed to induce this response. Pretreatment with ketotifen, a histamine H_1 receptor antagonist, and capsaicin inhibited LPA-induced ISRs. Additionally, LPA-induced ISRs were abolished by Y-27632, an inhibitor of Rho-associated protein kinase (ROCK). These findings suggest that LPA-induced ISRs are attributable to histamine- and substance-P-mediated pathways. Moreover, the Rho/ROCK-mediated pathway may be involved.

Introduction

Lysophosphatidic acid (LPA), the simplest of the water-soluble phospholipids, is produced in significant quantities by cell activation [1–3], a phenomenon that is suggestive of a possible role of LPA as a potent phospholipid mediator of diverse biological activities. Application of exogenous LPA to responsive cells induces various biological effects [4, 5]. Moreover, LPA can evoke enhancement of airway smooth muscle in vitro [6, 7]. Previously, we demonstrated the induction of airway hyperresponsiveness by LPA and infiltration of eosinophils and neutrophils in vivo; additionally, we described the role of LPA in histamine and superoxide release in vitro [8–10].

To a large extent, the LPA production appears to occur via hydrolysis of phospholipids following cell activation. Secretory phospholipase A_2 leads to the accumulation of various phospholipids. Furthermore, as a result of concomitant activation of phospholipase C or D and diacylglycerol kinase, phosphatidic acid accumulates. Phosphatidic acid is converted to LPA by secretory phospholipase A_2. Increased levels of secretory phospholipase A_2 are present in bronchoalveolar lavage fluid of sensitized guinea pigs and of antigen-challenged allergic asthmatics [11, 12]. On the basis of these observations, we hypothesized that LPA may contribute to the pathomechanisms of allergic disorders such as bronchial asthma.

KARGER

Fax +41 61 306 12 34
E-Mail karger@karger.ch
www.karger.com

0031–7012/04/0721–0051$21.00/0

Accessible online at:
www.karger.com/pha

Hisayuki Ohata
1-5-8 Hatanodai, Shinagawa-ku
Tokyo 142-8555 (Japan)
Tel. +81 3 3784 8212, Fax +81 3 3784 3232
E-Mail ohata@pharm.showa-u.ac.jp

Itch is an unpleasant sensation that provokes a desire to scratch. Itch is widely recognized as a major symptom in various allergic disorders such as atopic dermatitis [13], allergic conjunctivitis [14], and allergic rhinitis [15]. However, progress in terms of understanding of the pathophysiological mechanisms of itch has been hampered by the absence of a suitable model. Kuraishi et al. [16] in 1995 reported that subcutaneous injection of some pruritogenic agents into the rostral region of the back induced scratching behavior in mice; moreover, this scratching of the injection site was due to itch, and not to pain. Woodward et al. [17] in the same year also demonstrated that a conjunctival itch-scratch response (ISR) was produced by topical instillation of various pruritogenic agents in guinea pigs. It is currently accepted that these models will permit convenient, systematic characterization of the pharmacology of itch; additionally, antipruritic effects of various drugs were examined utilizing these models [18–20].

More recently, Renbäck et al. [21, 22] noted that LPA possessed nociception-producing activity on sensory neurons through substance P release from nociceptor endings [21] and through histamine release from mast cells [22]. These findings indicate that LPA is likely to induce ISRs in inflamed sites, as inflammatory mediators such as histamine, substance P, and prostaglandins (PGs) are responsible for itch [23].

The present study examined whether LPA induces ISRs in mice. Furthermore, in order to assess the precise mechanisms governing the LPA-induced ISR, the effects of ketotifen, a histamine H_1 receptor antagonist, capsaicin, and Y-27632, an inhibitor of Rho-associated protein kinase (ROCK), are described.

Materials and Methods

All experiments were conducted in accordance with the Guiding Principles for the Care and Use of Laboratory Animals approved by The Japanese Pharmacological Society.

Animals

Male ICR mice (Charles River Japan, Tokyo, Japan) weighing 26–36 g were used. The animals were maintained in an air-conditioned animal room at 23 ± 3°C, with 50 ± 20% relative humidity and a 12-hour light-dark cycle (lights on 08.00–20.00 h). The mice were fed a standard laboratory diet and provided with water ad libitum. Each group of mice consisted of 4–8 animals.

Materials

Monooleoyl phosphatidic acid monosodium (LPA) was obtained from Avanti Polar Lipids (Alabaster, Ala., USA). Additional reagents included the following: ketotifen fumarate (Sigma Chemical, St. Louis, Mo., USA), Y-27632 (Calbiochem-Novabiochem, Darmstadt, Germany), PGD_2 (Cayman Chemical, Ann Arbor, Mich., USA), histamine dihydrochloride (Wako Pure Chemical, Osaka, Japan), and capsaicin (Wako Pure Chemical).

LPA was dissolved in physiological saline, PGD_2 in 2% Na_2CO_3 and neutralized with 0.1 *N* HCl, and capsaicin was dissolved in physiological saline containing 10% ethanol and 10% Tween 80. The remaining reagents were prepared in physiological saline.

Behavioral Observation

Prior to the experiments, the hair of the rostral region of the back was shaved; furthermore, the animals were placed in an observation cage for acclimatization. LPA or another pruritogenic agent (50 µl) was administered intradermally into the rostral region of the back. Immediately after administration, the mice were again placed in an observation cage (3 animals/cage). The number of ISRs was monitored utilizing a video camera (Sony, Tokyo, Japan) equipped with a zoom lens according to the method of Kuraishi et al. [16], i.e., the scratching of the rostral region of the back with either hind limb was counted.

LPA-Induced ISRs

LPA (100 µg/site) and histamine (10 µg/site) were administered intradermally, and the ISRs were monitored as described above. The number of ISRs was counted every 10 min for 60 min following agent administration. When the dose-response relationship was examined, LPA (10 or 100 µg/site), histamine (1, 10, and 100 µg/site), and PGD_2 (100 and 1,000 µg/site) were administered; subsequently, the number of ISRs was counted for 30 min.

Roles of Histamine, Substance P, and ROCK in LPA-Induced ISRs

These studies were designed to determine the contribution, if any, of histamine, substance P, and ROCK with respect to the LPA-induced ISRs. For this purpose, 1 mg/kg of ketotifen or Y-27632 was administered intravenously. Five minutes after administration, 100 µg/site of LPA and 10 µg/site of histamine were administered intradermally; subsequently, the number of ISRs was monitored for 30 min. Several experiments involving capsaicin-treated animals were performed to clarify the involvement of substance P. Capsaicin desensitization was performed via administration of a total dose of 75 mg/kg s.c. over 2 days, as previously described [24].

Statistics

The values are expressed as mean ± SE. Student's t test or Dunnett's multiple-comparison test was employed to calculate the statistical significance of differences between the mean values of the test and control groups. $p < 0.05$ was considered statistically significant.

Results

LPA-Induced ISRs

Intradermal administration of LPA (100 µg/site) elicited scratching of the rostral region of the back with the hind limb (fig. 1); the effect peaked during the initial 10-

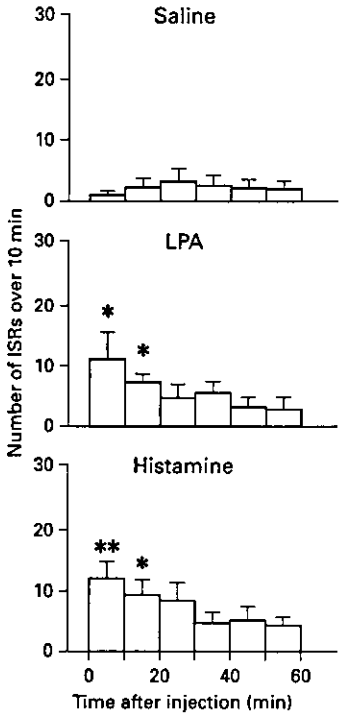

Fig. 1. Time course of ISRs induced by LPA and histamine in mice. LPA (100 μg/site) or histamine (10 μg/site) was administered intradermally into the rostral region of the back. The number of ISRs was observed and recorded every 10 min for 60 min following the injection. Each column represents the mean ± SE of 6 animals. Significantly different from the saline-treated group: * $p < 0.05$; ** $p < 0.01$ (Dunnett's multiple-comparison test).

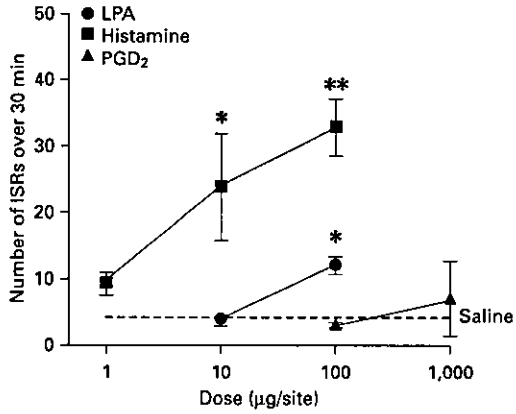

Fig. 2. Comparison of ISRs induced by LPA, histamine, and PGD_2 in mice. LPA, histamine, or PGD_2 was administered intradermally into the rostral region of the back. The number of ISRs was observed and recorded for 30 min. Each point represents the mean ± SE of 4–6 animals. Significantly different from the saline-treated group: * $p < 0.05$; ** $p < 0.01$ (Dunnett's multiple-comparison test).

min period. The number of ISRs during the initial 10-min period was 11.0 ± 4.13. The number of ISRs gradually decreased and nearly subsided by 30 min following administration; however, significant differences were evident between the LPA-treated and the saline-treated groups during the initial and the second 10-min period ($p < 0.05$). Histamine (10 μg/site) also induced ISRs similar to LPA; the peak number of ISRs was 11.7 ± 6.53. Statistically significant differences were observed with respect to the initial ($p < 0.01$) and the second ($p < 0.05$) 10-min period.

The dose-response relationship of LPA-induced ISRs is displayed in figure 2. The number of ISRs at 10 μg/site was 3.83 ± 0.95. No significant differences were detected in comparison with the saline-treated group. In contrast, 100 μg/site of LPA increased the ISR number (12.0 ± 1.32) for 30 min following agent administration. Histamine also induced ISRs in a dose-dependent manner; moreover, the numbers of ISRs at 1, 10, and 100 μg/site were 9.25 ± 1.70, 23.8 ± 8.02, and 32.8 ± 4.31, respectively. In addition, significant differences were observed at 10 μg/site ($p < 0.05$) and 100 μg/site ($p < 0.01$). However, PGD_2 failed to induce ISRs at 1,000 μg/site.

Effect of Ketotifen on LPA-Induced ISRs

Figure 3 presents the effects of ketotifen on LPA- and histamine-induced ISRs. The number of LPA-induced ISRs was 21.5 ± 4.70. Moreover, the value differed significantly from that of the saline-treated group ($p < 0.01$). Ketotifen, a histamine H_1 receptor antagonist, significantly lowered the LPA-induced number of ISRs to approximately one third of that of the vehicle-treated group. Significant differences were observed between the ketotifen- and the vehicle-treated groups ($p < 0.05$). Ketotifen substantially reduced the number of histamine-induced ISRs ($p < 0.05$).

Effect of Capsaicin Desensitization on LPA-Induced ISRs

The potential involvement of substance P in LPA-induced ISRs was investigated. The number of LPA-induced ISRs was 13.5 ± 3.48. Repeated treatment with capsaicin

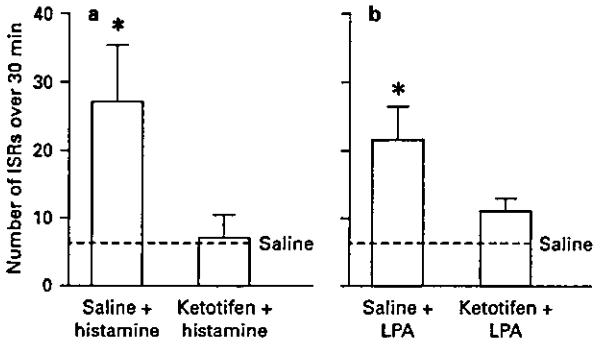

Fig. 3. Effects of ketotifen on ISRs induced by histamine (**a**) and LPA (**b**) in mice. Histamine (10 μg/site) or LPA (100 μg/site) was administered intradermally into the rostral region of the back. The number of ISRs was observed and recorded for 30 min. Ketotifen (1 mg/kg) was administered intravenously 5 min prior to histamine or LPA administration. Each column represents the mean ± SE of 5–6 animals. Significantly different from saline group: * $p < 0.05$ (Student's t test).

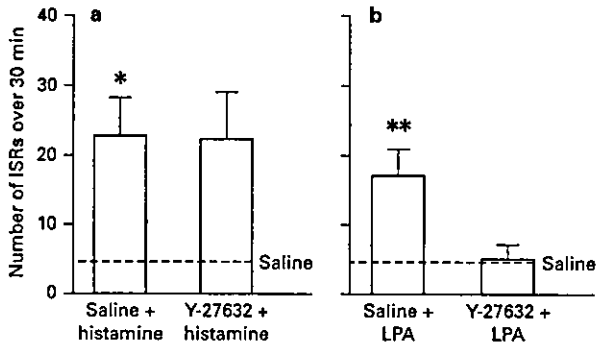

Fig. 5. Effects of Y-27632 on ISRs induced by histamine (**a**) and LPA (**b**) in mice. Histamine (10 μg/site) or LPA (100 μg/site) was administered intradermally into the rostral region of the back. The number of ISRs was observed and recorded for 30 min. Y-27632 (1 mg/kg) was administered intravenously 5 min prior to histamine or LPA administration. Each column represents the mean ± SE of 5–6 animals. Significantly different from the saline-treated group: * $p < 0.05$; ** $p < 0.01$ (Student's t test).

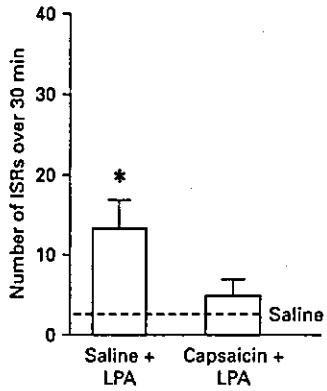

Fig. 4. Effects of capsaicin desensitization on the ISRs induced by LPA in mice. LPA (100 μg/site) was administered intradermally into the rostral region of the back. The number of ISRs was observed and recorded for 30 min. Capsaicin was administered subcutaneously into the caudal region of the back at increasing doses (25 and 50 mg/kg) daily for 2 days. Each column represents the mean ± SE of 5–6 animals. Significantly different from the saline-treated group: * $p < 0.05$ (Student's t test).

induced a significant inhibition of the ISR formation. Significant differences were evident between the capsaicin- and the vehicle-treated groups ($p < 0.05$; fig. 4).

Effect of Y-27632 on LPA-Induced ISRs

The effect of Y-27632 was examined (fig. 5). The LPA-induced number of ISRs was 16.7 ± 3.85; moreover, this value differed significantly from that of the saline-treated group ($p < 0.01$). The LPA-induced number of ISRs in the Y-27632-treated group was 4.83 ± 1.60. Moreover, the value differed significantly from that of the vehicle-treated group ($p < 0.05$). In contrast, Y-27632 scarcely affected the number of histamine-induced ISRs. No statistically significant differences were observed with respect to the vehicle-treated group.

Discussion

Afferent C fiber terminals in the skin are localized in the proximity to mast cells. These terminals, which are activated by various mediators produced by mast cells, transmit this information to sites, where it may cause the sensation of itch. Therefore, mast cells may play a key role in the pathophysiology of itching. In the present study, intradermal administration, consequent to its utility in numerous ISR experiments, was employed for the measurement of ISRs; furthermore, mast cells in the skin are distributed predominantly in the upper region of the dermis.

The results of the present study indicate that LPA causes ISRs in mice. We found that 100 μg/site of LPA induced ISRs. Moreover, the maximum effect was observed during the initial 10-min period; this effect nearly subsided by 30 min following LPA administration. Consequently, the number of ISRs was monitored for 30 min. LPA at 10 μg/site failed to exert any effect; however, the ISRs induced by LPA at 100 μg/site were of a considerable magnitude.

Diluted formalin (5 mg formaldehyde) applied to the rostral region of the back did not induce ISRs [16]. Acetic acid (10 mmol/l) produced no meaningful ISRs in guinea pig eyes [17]. Inagaki et al. [18] also noted that ISRs in mice may be induced by a sensation or a mechanism similar to itching in humans; moreover, these authors concluded that this model was suitable for the examination of itching in humans. On the basis of these findings, we hypothesize that the ISR does not occur in response to pain-related and foreign body stimuli. Hence, it appears likely that the LPA-induced ISR is due to itch and not to pain. To the best of our knowledge, this is the first report demonstrating LPA-induced ISRs.

PGD_2 and PGE_2 appear to possess pruritogenic activity in the guinea pig eye [17]. Despite this finding, the ISR was not induced by intradermal administration of PGD_2. Greaves and McDonald-Gibson [25] noted that PGE_2 itself did not cause itching; however, it did lower the threshold of the skin to itching provoked by histamine as well as by other mediators. The present findings with respect to the absence of induction of ISR suggest that PGD_2 may act synergistically to promote ISRs.

In the present study, ketotifen and capsaisin were shown to exert inhibitory effects on the LPA-induced ISRs. These results indicate that the release of histamine and substance P was involved in LPA-induced ISRs. Histamine is well established as a classical pruritogenic substance [26]. There is evidence regarding the ability of substance P to create an itch sensation in humans when applied to the skin [27]. Hence, we hypothesize that LPA, in addition to histamine and other mediators, may induce an itch sensation in humans.

Although it is well known that substance P induces histamine release [28], we hypothesize that the histamine-mediated pathway is not identical to the substance-P-mediated pathway in LPA-induced ISRs. In the present study, ketotifen partially inhibited LPA-induced ISRs; however, this substance abolished histamine-induced ISRs. If substance P contributes to the development of LPA-induced ISRs via the histamine-mediated pathway, the LPA-induced ISRs should disappear upon treatment with ketotifen. Schmelz et al. [29] reported that endogenously released substance P did not degranulate mast cells in the healthy human skin. Andoh and Kuraishi [30] also reported that substance-P-induced scratching was not suppressed by chlorpheniramine and that intradermal administration of substance P increased the cutaneous concentrations of leukotriene B_4. Substance P induced by LPA may not cause the release of histamine; other mediators, such as leukotriene B_4, may be involved.

LPA-induced ISRs displayed a marked inhibition upon treatment with 1 mg/kg of Y-27632, an inhibitor of ROCK. This finding was indicative of the involvement of the Rho/ROCK-mediated pathway in LPA-induced ISRs. The relations between the Rho/ROCK-mediated pathway and the histamine- or substance-P-mediated pathway were not clarified in the present study. We hypothesize that the Rho/ROCK-mediated pathway was not involved in the activation of C fibers by the histamine released; moreover, this pathway did not influence the transmission of the itch sensation to the central nervous system, as Y-27632 failed to attenuate histamine-induced ISRs. The Rho/ROCK-mediated pathway may participate in the release of histamine and substance P.

To summarize, we conclude that LPA induces ISRs; furthermore, our findings suggest that LPA-induced ISRs may be attributable to the histamine-, substance-P-, and Rho/ROCK-mediated pathways. This effect indicates the potential role of LPA in terms of its contribution to itch accompanying allergic disorders such as atopic dermatitis, allergic conjunctivitis, and allergic rhinitis.

References

1 Watson SP, McConnell RT, Lapetina EG: Decanoyl lysophosphatidic acid induces platelet aggregation through an extracellular action: Evidence against a second messenger role for lysophosphatidic acid. Biochem J 1985;232:61–66.

2 Bocckino SB, Blackmore PF, Wilson PB, Exton JH: Phosphatidate accumulation in hormone-treated hepatocytes via a phospholipase D mechanism. J Biol Chem 1987;262:15309–15315.

3 Gerrard JM, Robinson P: Identification of the molecular species of lysophosphatidic acid produced when platelets are stimulated by thrombin. Biochim Biophys Acta 1989; 1001:282–285.

4 Moolenaar WH: Lysophosphatidic acid signalling. Curr Opin Cell Biol 1995;7:203–210.

5 Rizza C, Leitinger N, Yue J, Fischer DJ, Wang DA, Shih PT, Lee H, Tigyi G, Berliner JA: Lysophosphatidic acid as a regulator of endothelial/leukocyte interaction. Lab Invest 1999; 79:1227–1235.

6 Toews ML, Ustinova EE, Schultz HD: Lysophosphatidic acid enhances contractility of isolated airway smooth muscle. J Appl Physiol 1997;83:1216–1222.

7 Sakai J, Oike M, Hirakawa M, Ito Y: Theophylline and cAMP inhibit lysophosphatidic acid-induced hyperresponsiveness of bovine tracheal smooth muscle cells. J Physiol 2003;549(Pt 1):171–180.

8 Hashimoto T, Nakano Y, Ohata H, Momose K: Lysophosphatidic acid enhances airway response to acetylcholine in guinea pigs. Life Sci 2001;70:199–205.

9 Hashimoto T, Nakano Y, Yamashita M, Fang YI, Ohata H, Momose K: Role of Rho-associated protein kinase and histamine in lysophosphatidic acid-induced airway hyperresponsiveness in guinea pigs. Jpn J Pharmacol 2002;88:256–261.

10 Hashimoto T, Yamashita M, Ohata H, Momose K: Lysophosphatidic acid enhances in vivo infiltration and activation of guinea pig eosinophils and neutrophils via a Rho/Rho-associated protein kinase-mediated pathway. J Pharmacol Sci 2003;91:8–14.

11 Sane AC, Mendenhall T, Bass DA: Secretory phospholipase A_2 activity is elevated in bronchoalveolar lavage fluid after ovalbumin sensitization of guinea pigs. J Leukoc Biol 1996; 60:704–709.

12 Bowton DL, Seeds MC, Fasano MB, Goldsmith B, Bass DA: Phospholipase A_2 and arachidonate increase in bronchoalveolar lavage fluid after inhaled antigen challenge in asthmatics. Am J Respir Crit Care Med 1997; 155:421–425.

13 Lorette G, Vaillant L: Pruritus: Current concepts in pathogenesis and treatment. Drugs 1990;39:218–223.

14 Bielory L, Goodman PE, Fisher EM: Allergic ocular disease: A review of pathophysiology and clinical presentations. Clin Rev Allergy Immunol 2001;20:183–200.

15 Cook PR: Seasonal allergic rhinitis. Mo Med 1996;93:247–250.

16 Kuraishi Y, Nagasawa T, Hayashi K, Satoh M: Scratching behavior induced by pruritogenic but not algesiogenic agents in mice. Eur J Pharmacol 1995;14:229–233.

17 Woodward DF, Nieves AL, Spada CS, Williams LS, Tuckett RP: Characterization of a behavioral model for peripherally evoked itch suggests platelet-activating factor as a potent pruritogen. J Pharmacol Exp Ther 1995; 272:758–765.

18 Inagaki N, Nakamura N, Nagao M, Kawasaki H, Nagai H: Inhibition of passive cutaneous anaphylaxis-associated scratching behavior by mu-opioid receptor antagonist in ICR mice. Int Arch Allergy Immunol 2000;123:365–368.

19 Fukuda S, Midoro K, Yamasaki M, Gyoten M, Kawano Y, Fukui H, Ashida Y, Nagaya H: Characteristics of the antihistamine effect of TAK-427, a novel imidazopyridazine derivative. Inflamm Res 2003;52:206–214.

20 Woodward DF, Nieves AL, Friedlaender MH: Characterization of receptor subtypes involved in prostanoid-induced conjunctival pruritus and their role in mediating allergic conjunctival itching. J Pharmacol Exp Ther 1996; 279:137–142.

21 Renbäck K, Inoue M, Ueda H: Lysophosphatidic acid-induced, pertussis toxin-sensitive nociception through a substance P release from peripheral nerve endings in mice. Neurosci Lett 1999;270:59–61.

22 Renbäck K, Inoue M, Yoshida A, Nyberg F, Ueda H: Vzg-1/lysophosphatidic acid-receptor involved in peripheral pain transmission. Brain Res Mol Brain Res 2000;75:350–354.

23 Greaves MW, Wall PD: Pathophysiology of itching. Lancet 1996;348:938–940.

24 Morris JB, Symanowicz PT, Olsen JE, Thrall RS, Cloutier MM, Hubbard AK: Immediate sensory nerve-mediated respiratory responses to irritants in healthy and allergic airway-diseased mice. J Appl Physiol 2003;94:1563–1571.

25 Greaves MW, McDonald-Gibson W: Itch: Role of prostaglandins. Br Med J 1973;3:608–609.

26 Davies MG, Greaves MW: The current status of histamine receptor in human skin: Therapeutic implications. Br J Dermatol 1981; 104:601–606.

27 Hägermark Ö, Hökfelt T, Pernow B: Flare and itch induced by substance P in human skin. J Invest Dermatol 1978;71:233–235.

28 Erjavec F, Lembeck F, Florjanc-Irman T, Skofitsch G, Donnerer J, Saria A, Holzer P: Release of histamine by substance P. Naunyn Schmiedebergs Arch Pharmacol 1981;317:67–70.

29 Schmelz M, Zeck S, Raithel M, Rukwied R: Mast cell tryptase in dermal neurogenic inflammation. Clin Exp Allergy 1999;29:695–702.

30 Andoh T, Kuraishi Y: Inhibitory effects of azelastine on substance P-induced itch-associated response in mice. Eur J Pharmacol 2002; 436:235–239.

日薬理誌（*Folia Pharmacol. Jpn.*）**124**，329～335（2004）

メカノセンシタイザーとしてのリゾホスファチジン酸の役割

大幡　久之，新岡　丈治，金　　明淑，
安藤さなえ，山本　雅幸，百瀬　和享

要約：細胞は，液性・化学因子に加えて，機械的，物理的因子を刺激として受容し，様々な細胞応答を起こす．例えば，血流の局所的な制御には，血流刺激による血管内皮細胞からの血管トーヌス制御因子の放出が重要な役割を果たしている．しかし，これらの機械刺激の感知機構の実体は未だに不明である．著者らは，生体活性リン脂質の一つであるリゾホスファチジン酸（LPA）が培養平滑筋細胞や培養水晶体上皮細胞などと同様に培養ウシ大動脈血管内皮細胞の流れ刺激により誘発されるCa^{2+}応答を著明に増強することをリアルタイム共焦点顕微鏡を用いて画像化することにより明らかにした．この時認められるCa^{2+}応答は，機械受容チャネルからのCa^{2+}流入とその拡散による局所的なCa^{2+}上昇から成る時空的特徴を持つ現象であり，機械受容応答の初期過程に直結したエレメンタリーイベントとしてCa^{2+} spotsと命名した．この現象が血流中に存在しうるLPA濃度と生理的な流れ刺激強度の範囲で生じることから，LPAが機械受容機構の内因性の制御因子である可能性が示唆された．また，最近，組織構築を維持したマウス大動脈中の内皮細胞においてもほぼ同様の現象が生じることを確認し，上皮細胞や内皮細胞で認められる普遍的な現象であると考えられた．本稿ではLPAが機械受容応答の感受性を増強する内因性物質（メカノセンシタイザー）として機能する可能性を示し，さらにはその生理的病態生理学的意義について考察する．

1. はじめに

細胞は，神経伝達物質，ホルモン，細胞増殖因子，イオンや薬物などの液性・化学因子に加えて，機械的，物理的因子を刺激として受容し，様々な細胞応答を起こすことが明らかとなっている．例えば，循環器系は，神経性支配とホルモン性の制御により，全身性に，さらには臓器レベルで制御されているが，これらだけでは身体の隅々まで血流をきめ細かく制御することは難しい．この局所における血液循環の恒常性維持において，血液の流れに伴うずり応力や伸展刺激などを内皮細胞が感知して一酸化窒素などの血管トーヌス制御因子を産生・放出する機構が重要な役割を果たしている(1)．また，このような短期的な循環制御に加えて，内皮細胞の流れ刺激受容機構は血流変化に適応した血管径の変化（リモデリング）のような長期的な変化や内膜肥厚や粥状動脈硬化症などの病態発現にも関与することが知られている(2)．このように内皮細胞の機械受容機構は，循環制御において生理学的・病態生理学的に極めて重要な役割を果たしている．しかしながら，その初期過程である流れ刺激受容機構については，本ミニ総説号の中でも他の著者らによって示されているようないくつかの仮説が提唱されているものの，統一した見解は得られておらず，機械受容分子の実体も未だ明らかではないのが現状である．

著者らは，細胞間情報伝達物質として注目されるリゾホスファチジン酸（LPA）が消化管平滑筋細胞，肺上皮細胞および水晶体上皮細胞の機械刺激によるカルシウム応答を顕著に促進することを報告してきた(3～5)．さらに，最近，培養内皮細胞においてもLPA存在下で流れ刺激強度に依存し，時空的にも特徴的な性質を有するカルシウム応答（Ca^{2+} spot）を生じることを見いだした(6)．LPAは正常血漿中に存在し，血小板の活性化によって遊離されることや多発性骨髄腫などの疾患時に血漿中に増加すること(7～9)から，LPAが機械受容応答の感受性を増強する内因性物質（メカノセンシタイザー）であるという仮説を提唱している(10)．本稿では，LPAのメカノセンシタイザーとしての性質と生理学的および病態生理学的意義について述べたい．

キーワード：リゾホスファチジン酸，機械受容機構，
機械受容チャネル，
細胞内カルシウムイオン濃度
昭和大学薬学部薬理学教室
（〒142-8555 東京都品川区旗の台1-5-8）
e-mail: ohata@pharm.showa-u.ac.jp
原稿受領日：2004年7月26日，編集委員会依頼総説

2. LPAの機械受容応答促進作用の発見

はじめに，LPAが機械受容応答促進作用を有することを見いだした経緯について触れたい．著者らは以前に細胞内情報伝達系の一員としてのホスファチジン酸の作用に着目して検討を行っており，平滑筋収縮作用を有することを報告してきたが，そのリゾ体であるリゾホスファチジン酸（LPA）も細胞間情報伝達物質として様々な生理活性を有することが明らかとなりつつあり，その作用メカニズムとして培養平滑筋細胞のカルシウム動態を指標として検討を行った．培養平滑筋細胞において，LPAは比較的低濃度（10 nM）から適用により一過性あるいは反復性のカルシウム応答を引き起こしたが，LPA存在下にカルシウム上昇を起こすとは考えられない試薬の適用により一過性のカルシウム応答が観察された．繰り返し同様の操作を行っても再現するが，LPAが存在しなければカルシウム上昇は生じないことから，試薬を加えないで撹拌だけを行ったところ，同様のカルシウム上昇を起こすことが確認された．細胞は機械的な刺激にも応答することは，平滑筋の伸展刺激や内皮細胞への流れ刺激時の応答などでよく知られていることではあったが，正直なところそれまでは研究の対象として考えることはなかった．この現象がLPA存在下で起こる特異的なものであるとするなら，LPAは細胞の機械受容応答を促進する作用があるのではないかと考えたのが，この研究の出発点である．はじめにLPAの両親媒性物質としての作用が膜の性質を変化させた結果として生じた現象である可能性を想定して，LPAより界面活性作用が強いリゾホスファチジルコリン（LPC）の作用と比較検討したところ，LPCも機械刺激によるカルシウム応答を僅かに促進したが，その濃度はLPAの100倍程度を必要としたことから，この作用はLPAによる特異的な作用であると考えられた．また，機械受容チャネルの阻害物質としてよく用いられるガドリニウムによってこのカルシウム応答が抑制されたことから，LPAは機械刺激に伴う機械受容チャネルの活性化を介するカルシウム応答を増強する可能性が考えられた．これらの結果から，LPAが機械受容応答の感受性を増強する内因性物質（メカノセンシタイザー）であるという仮説を初めて報告した(3)．

培養平滑筋細胞で認められたLPAの作用は，その後，培養肺上皮細胞(4)や培養ウシ水晶体上皮細胞(5)においても認められることを明らかにした．水晶体上皮細胞では，micromolar levelのLPAを必要とし，そのカルシウム応答の性質は培養平滑筋細胞で認められた性質と一部異なり，LPAの適用時のカルシウム応答はほとんど見られないが機械刺激による顕著なカルシウム上昇が観察された．また，このカルシウム上昇は外液カルシウム濃度依存性が高く，小胞体カルシウムポンプ阻害薬のタプシガルジン前処置下においても認められることから，LPAは機械受容チャネルを介するカルシウム流入を増強することが強く示唆された．

3. Ca^{2+} spot現象

これまで述べてきたLPAによる機械刺激に伴うカルシウム応答の増強作用は，通常の共焦点レーザー走査型顕微鏡を用いたカルシウムイメージングにより得られた結果であり，その時間分解能は秒単位のものであり，細胞レベルでのカルシウム応答あるいは細胞内での濃度分布の変化を詳細に検討するには十分な時間分解能とは言えなかった．このLPAによって増強されるカルシウム応答については，機械受容応答を促進する物質としてのLPAの作用メカニズムに興味が持たれるところであるとともに，機械刺激に依存したカルシウム上昇の経路についても非常に興味深い．何故なら，機械受容分子の実態は明らかではなく，また，受容分子の候補とされる機械受容チャネルも電気生理学的に証明されているものの，その分子実態は明らかではない(11～13)．この点においても，LPAが機械受容チャネルの活性を高める作用があるとすれば，このカルシウム応答を詳細に検討することにより何らかの情報が得られることが期待された．そこで，同時期に導入されたマルチピンホールタイプのニポウディスク走査型共焦点スキャナーと高速冷却CCDカメラ蛍光イメージングシステムを組み合わせた高速高分解能画像化法を用いて培養水晶体細胞でのLPA存在下で生じる機械刺激に依存したカルシウム応答を詳細に検討した．このシステムは，ビデオレート（30フレーム／秒）よりさらに高い時間分解能を有することから，細胞内で生じるカルシウムウエーブやさらにはカルシウムスパーク(14, 15)などのチャネル単位のカルシウム応答をとらえることが可能である．著者らは当初，これまでの薬理学的な検討から，カルシウムの上昇は細胞膜付近から始まり細胞内へと拡散するような画像が得られることを予想していた．しかし，初めてこのシステムを用いて得られた画像はそれとは異なり，今までに見たこともない光の瞬くような綺麗なカルシウム応答であった．水晶体上皮細胞の数カ所（多いときには数十カ所）の直径数μmの局所からわずかな時間差をもって起こる急激なカルシウム上昇が同心円状に広がってゆく現象であった．この現象はカルシウムスパークとはその持続時間において大きく異なり，持続的に拡散してゆく現象であり，また，カルシウムウェーブとも異なり，その上昇速度は開始部位で最も高く，開始部位からの距離に反比例して低くなること，タプシガルジン存在下でも有意な影響を受けないことから，特定の部位から流入したカルシウムが単純に細胞内を拡散する現象

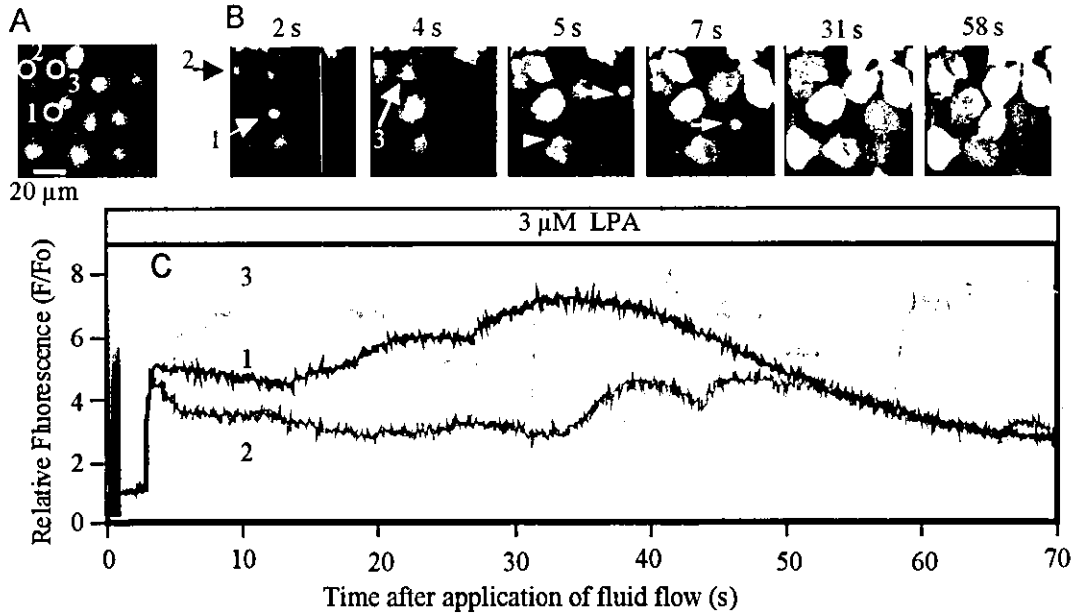

Fig. 1 Ca^{2+} response in aortic endothelial cells to fluid flow in the presence of LPA. Cells were stimulated by fluid flow in the presence of 3 μM LPA. A: fluo-4 fluorescence image in the resting state, B: ratio images during application of fluid flow, C: time course of Ca^{2+} response to fluid flow in three different regions shown in B.

であると推定された．また，ガドリニウムによって抑制されることから，少数単位の機械受容チャネルを介するカルシウム流入を初めて画像としてとらえたものであり，機械受容応答に直結したカルシウム応答として Ca^{2+} spot と命名した(6, 16)．

機械受容応答がその細胞機能の発現において重要な役割を担う細胞として，血管内皮細胞が挙げられる．著者らは水晶体上皮細胞の実験に引き続いて培養ウシ大動脈内皮細胞を用いて LPA 存在下流れ刺激によるカルシウム応答について検討を行った．その結果，ほぼ同様の薬理学的，時空的性質を示す Ca^{2+} spot 現象をとらえることに成功した(Fig. 1) (6)．

Ca^{2+} spot は細胞膜で生じる局所的なカルシウム流入現象である．そこで，次にこの現象が細胞の機械刺激を直接受ける自由膜面で生ずる現象かあるいは基底膜面で生じる現象かという点に興味が持たれた．これまでの実験においても共焦点レーザー走査顕微鏡を用いて画像化を行っていたが，細胞の厚みは最も厚いところでも 10 μm 以下であり，共焦点レーザー走査顕微鏡の光軸分解能が約 1 μm としても，Ca^{2+} spot は瞬時に広がって行ってしまうため，どちらの膜面に焦点を合わせて画像を取得しても，個々の Ca^{2+} spot の時空的特性はそれらのバラツキの範囲内に収まってしまい，その区別は困難である．そこで同時期に開発を進めていた高速高分解能四次元画像化システム(17)を用いて細胞の基底膜面と自由膜面におけるカルシウム動態を同時に画像化することにより検討した．このシステムは細胞の基底膜面と自由膜面の画像を 9.4 msec の時間差で画像化ことが可能であり，同一の Ca^{2+} spot を基底膜面と自由膜面において同時に観察することができる．はじめに培養水晶体上皮細胞で検討した結果，Fig. 2 に示すように細胞へ辺縁部分の厚みのない部分で生じる Ca^{2+} spot では区別することが困難であったが，細胞の厚みのある核の部分では自由膜面で Ca^{2+} spot（矢印）が生じることが明らかとなった．また，ウシ大動脈内皮細胞においても同様の実験を行ったところ，やはり，自由膜面で基底膜面よりカルシウム濃度上昇速度が大きな明瞭な Ca^{2+} spot が観察され（Fig. 3），細胞が直接刺激を受ける自由膜面に存在する機械受容チャネルを介するカルシウムの流入とその拡散により生じる現象であると考えられた．機械受容チャネルは電気生理学的にその存在が示されているのみで，タンパク質レベルおよび遺伝子レベルでは未だに未知の細胞外膜チャネルであることから，このチャネルの開口に伴うエレメンタリーイベントと考えられる Ca^{2+} spot の検出は，機械感受性チャネルとしての実体に迫るものとして評価され，

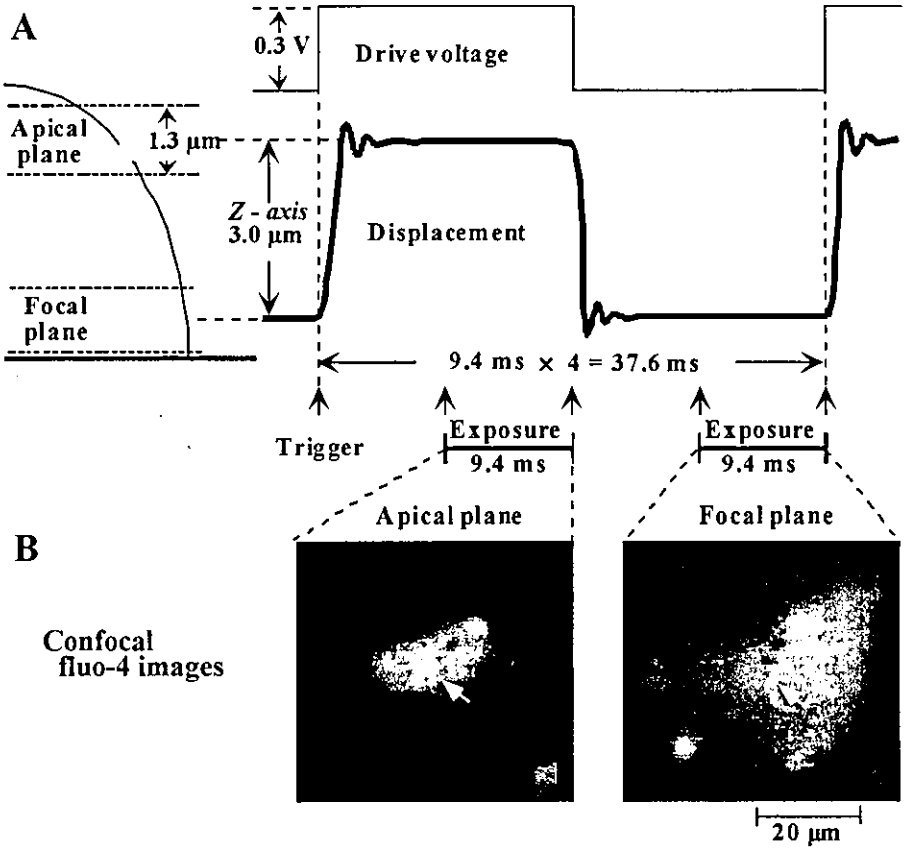

Fig. 2 Simultaneous confocal imaging of Ca^{2+} spots at apical and focal planes of lens epithelial cells using the high-speed three-dimensional confocal imaging system. A: Relationship between changes in Z-axis position with the Microscope Objective NanoPositioner controlled by electrical square waves and camera exposure. The detailed protocol is described in the text. B: Confocal fluorescence images of fluo-4-loaded neuronal cell (upper) and astroglial cells (lower) obtained by this confocal system.

Circ Res 88(9)，2001 の表紙に採用された．

4. 生理学的および病態生理学的意義

これまでの結果は全て培養細胞を用いて得られたものであるため，LPA の流れ刺激受容応答の促進作用が実際に生体内で起こりうる現象であるか否かについては，より生体内環境に近い組織標本を用いた検討が必要と考えられた．そこで，自作した平行平板型流れ刺激負荷装置に摘出したマウス大動脈組織標本を固定して栄養液を一定流量で還流することで内皮細胞に流れ刺激を負荷し，この時の Ca^{2+} 動態を多光子励起レーザー顕微鏡を用いて可視化した．この画像化システムを用いることにより，約 1 秒間に 1 画像を取得し，約 10 分間の連続的な Ca^{2+} 動態を同一視野で 4,5 回繰り返して可視化することが可能であった．このように繰り返し同一視野で長時間の観察が可能となったのは，多光子励起レーザー顕微鏡を用いたことによる細胞へのフォトダメージの軽減が大きく寄与しているものと考えられた(18)．この検討の結果，LPA はマウス大動脈標本においても培養ウシ大動脈内皮細胞で認められたものと同一の流れ刺激依存性の Ca^{2+} 流入現象を引き起こすことが明らかとなった．特に，その特徴的時空的特性や外液 Ca^{2+} 依存性だけでなく，LPA 濃度依存性（0.3～10 μM）および流れ刺激強度依存性が培養ウシ大動脈内皮細胞での結果とほぼ同一であることは非常に興味深い（未発表）．また，同一の実験系を用いて機械刺激時にカルシウム応答を引き起こす内因性物質として注目される ATP(19)と比較検討した．ATP はその濃度依存的に Ca^{2+} 応答を促進したものの，LPA 存在下でみられるような流れ刺激依存性は示さなかった．この結果は，LPA の作用が内皮細胞に対して普遍的なものであり，この現象を引き起こす LPA 濃度と流れ

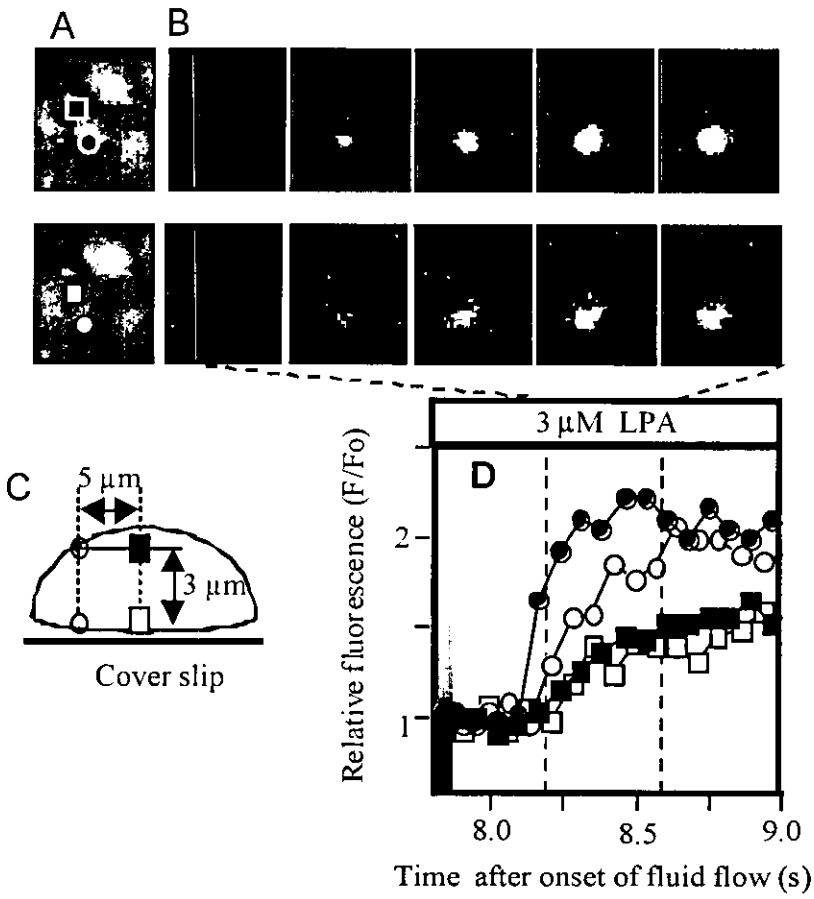

Fig. 3 Simultaneous confocal imaging of fluid flow-induced Ca^{2+} response at apical and focal planes of endothelial cells. Cells were stimulated by fluid flow in the presence of 3 μM LPA. A: fluo-4 fluorescence images in the resting state at apical (upper image) and focal planes (lower image), B: successive ratio images of localized Ca^{2+} response at apical and focal planes, C: regions analyzed quantitatively at apical and focal planes, D: time course of Ca^{2+} responses to fluid flow in the starting region and an adjacent region shown in A and C.

刺激強度が生体内で変化しうる範囲にあることから生体内で起こりうる現象であることを裏付けている．また，LPAはATPと対比した場合にも内皮細胞の流れ刺激感受性に影響を与える重要な生体物質であることを示していると考えられる．

さらに最近，シェアストレス存在下LPAにより誘発されるカルシウム応答と，それに引き続く血管組織の収縮応答について検討を行ったところ，内皮細胞のカルシウム上昇に数秒遅れて平滑筋細胞のカルシウム上昇と収縮反応を示す平滑筋細胞の長軸走行に沿った短縮を画像として捉えている（未発表）．

LPAは正常ヒト血漿中にsubmicromolar levelで存在し(7)，細胞間情報伝達物質として機能することが示唆されている．また，多発性骨髄腫(9)や卵巣癌(20)の患者血漿濃度は高値を示し，粥状動脈硬化症病変部位に蓄積されることが報告され(21)，血小板活性化や炎症により増加することが予想されている(8)．Ca^{2+} spotは，LPAの存在下で検出できた現象であるが，生理学的・病態生理学的なLPA濃度範囲で増強されることから，生体内でLPAが機械受容応答を左右する生理活性脂質として機能する可能性は大きいと考えられる．

5. おわりに

LPAは，多彩な生理活性を有する生体リゾリン脂質であり，血管系においても血管透過性(22)や血管リモデリング(23)に関与する可能性が示されている．本稿で述べた

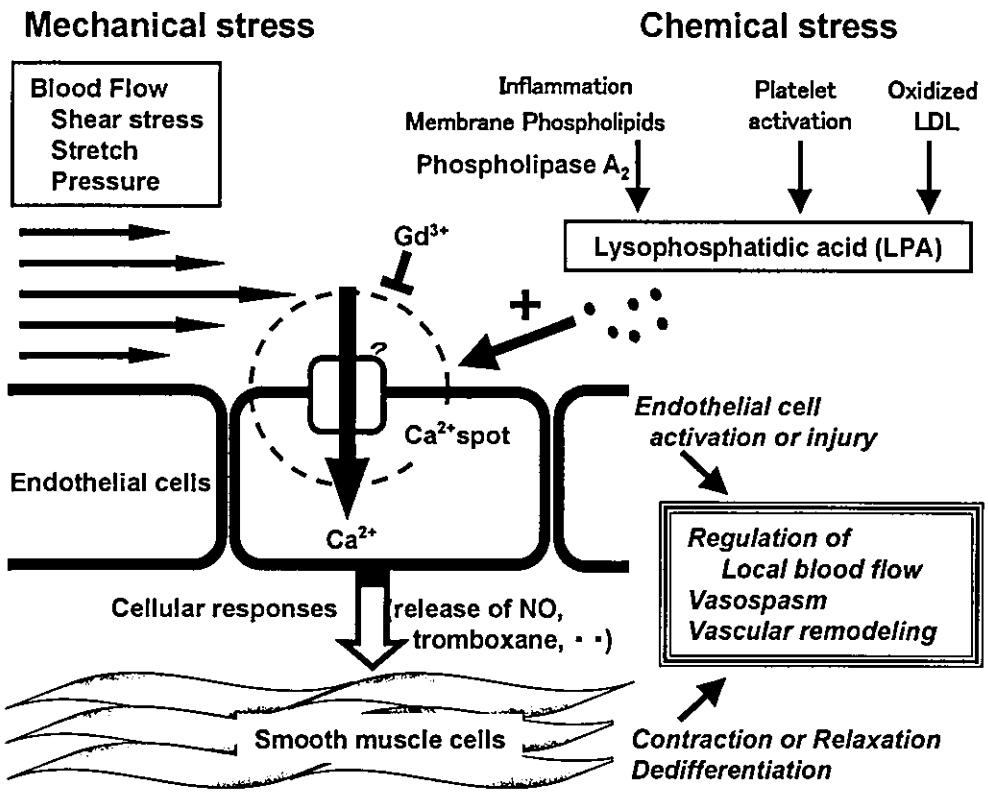

Fig. 4 Possible contribution of LPA as mechanosensitizer in endothelial cell-related vascular function and abnormality.

LPAの機械受容応答の増強作用は，血管内皮細胞の流れ刺激の変化に依存して生じる細胞応答に少なからず影響を与える可能性を示しており，これまで報告されている内皮細胞に対する作用の一部は，この機械受容応答の促進作用に基づく作用である可能性も考えられる．LPAは，submicromolar levelでは内皮依存的な血管トーヌス制御に関わる可能性があり，高濃度域では前述のような内皮依存的な血管収縮反応や内皮細胞障害による様々な血管障害に関わる可能性が考えられる（Fig. 4）．今後，LPAによる機械受容応答促進作用の詳細なメカニズムを明らかにするとともに，マウス大動脈で観察されたLPAにより生じる内皮依存的な血管収縮反応がその他の部位の血管にも認められるか否か，さらには冠血管や脳血管で生じるスパスムや内皮依存性弛緩反応の減弱などとの関連性についても興味が持たれるところであり，詳細な検討を進める予定である．

文　献

1) Davies PF. Flow-mediated endothelial mechanotransduction. Physiol Rev. 1995;75:519-560.
2) Gimbrone MA Jr, Topper JN. Molecular basis of cardiovascular disease. Philadelphia, Pa: WB Sanders;1999. p. 331-348.
3) Ohata H, Seito N, Aizawa H, Nobe K, Momose K. Sensitizing effect of lysophosphatidic acid on mechanoreceptor-linked response in cytosolic free Ca^{2+} concentration in cultured smooth muscle cells. Biochem Biophys Res Commun. 1995;208:19-25.
4) Ohata H, Seito N, Yoshida K, Momose K. Lysophosphatidic acid sensitizes mechanical stress-induced Ca^{2+} mobilization in cultured human lung epithelial cells. Life Sci. 1996;58:29-36.
5) Ohata H, Tanaka K, Aizawa H, Ao Y, Iijima T, Momose K. Lysophosphatidic acid sensitises Ca^{2+} influx through mechanosensitive ion channels in cultured lens epithelial cells. Cell Signal. 1997;9:609-616.
6) Ohata H, Ikeuchi T, Kamada A, Yamamoto M, Momose K. Lysophosphatidic acid positively regulated the fluid flow-induced local Ca^{2+} influx in bovine aortic endothelial cells. Circ Res. 2001;88:925-932.
7) Tigyi G, Miledi R. Lysophosphatidates bound to serum albumin activate membrane currents in *Xenopus* oo-

cytes and neurite retraction in PC12 pheochromocytoma cells. J Biol Chem. 1992;267:21360-21367.
8) Eichholtz T, Jalink K, Fahrenfort I, Moolenaar WH. The bioactive phospholipid lysophosphatidic acid is released from activated platelets. Biochem J. 1993;29:677-680.
9) Sasagawa T, Okita M, Murakami J, Kato T, Watanabe A. Abnormal serum lysophospholipids in multiple myeloma patients. Lipids. 1999;34:17-21.
10) Ohata H, Tanaka K, Maeyama N, Ikeuchi T, Kamada A, Yamamoto M, et al. Physiological and pharmacological role of lysophosphatidic acid as modulator in mechanotransduction. Jpn J Pharmacol. 2001;87:171-176.
11) Morris CE. Mechanosensitive ion channels. J Membr Biol. 1990;113:93-107.
12) Naruse K, Sokabe M. Involvement of stretch-activated ion channels in Ca^{2+} mobilization to mechanical stretch in endothelial cells. Am J Physiol. 1993;264:C1037-C1044.
13) Yao X, Kwan HY, Chan FL, Chan NW, Huang Y. A protein kinase G-sensitive channel mediates flow-induced Ca^{2+} entry into vascular endothelial cells. FASEB J. 2000;14:932-938.
14) Cheng H, Lederer WJ, Cannell MB. Calcium sparks: elementary events underlying excitation-contraction coupling in heart muscle. Science. 1993;262:740-744.
15) Nelson MT, Cheng H, Rubart M, Santana LF, Bonev AD, Knot HJ, et al. Relaxation of arterial smooth muscle by calcium sparks. Science. 1995;270:633-637.
16) Ohata H, Tanaka T, Maeyama N, Yamamoto M, Momose K. Visualization of elementary mechanosensitive Ca^{2+}-influx events, Ca^{2+} spots, in bovine lens epithelial cells. J Physiol (Lond). 2001;532:31-42.
17) Ohata H, Yamamoto M, Ujike Y, Rie G, Momose K. Confocal imaging analysis of intracellular ions in mixed cellular systems or in situ using two types of confocal microscopic systems. Methods Enzymol. 1999;307:425-441.
18) Ohata H, Yamada H, Niioka T, Yamamoto M, Momose K. Calcium imaging in blood vessel *in situ* employing two-photon excitation fluorescence microscopy. J Pharmacol Sci. 2003;93:242-247.
19) Yamamoto K, Korenaga R, Kamiya A, Ando J. Fluid shear stress activates Ca^{2+} influx into human endothelial cells via P2X4 purinoceptors. Circ Res. 2000;87:385-391.
20) Xu Y, Shen Z, Wiper DW, Wu M, Morton RE, Elson P, et al. Lysophosphatidic acid as a potential biomarker for ovarian and other gynecologic cancers. JAMA. 1998;280:719-723.
21) Siess W, Zangl KJ, Essler M, Bauer M, Brandl R, Corrinth C, et al. Lysophosphatidic acid mediates the rapid activation of platelets and endothelial cells by mildly oxidized low density lipoprotein and accumulates in human atherosclerotic lesions. Proc Natl Acad Sci USA. 1999;96:6931-6936.
22) Alexander JS, Patton WF, Christman BW, Cuiper LL, Haselton FR. Platelet-derived lysophosphatidic acid decreases endothelial permeability in vitro. Am J Physiol. 1998;274:H115-H122.
23) Yoshida K, Nishida W, Hayashi K, Ohkawa Y, Ogawa A, Aoki J, et al. Vascular remodeling induced by naturally occurring unsaturated lysophosphatidic acid in vivo. Circulation. 2003;108:1746-1752.

Abstract – Role of lysophosphatidic acid as a mechanosensitizer. Hisayuki OHATA, Takeharu NIIOKA, Myung-sook KIM, Sanae ANDO, Masayuki YAMAMOTO, and Kazutaka MOMOSE (Department of Pharmacology, School of Pharmaceutical Sciences, Showa University, Hatanodai, Shinagawa-ku, Tokyo 142-8555, Japan)
Folia Pharmacol. Jpn. (Nippon Yakurigaku Zasshi) **124**, 329～335 (2004)
The mechanotransduction mechanisms play an important role in regulation of specific cellular response or maintenance of cellular homeostasis in a wide variety of cell types. Increase in intracellular free Ca^{2+} concentration ($[Ca^{2+}]_i$) is an important signal in the first step of mechanotransduction. Mechanosensitive (MS) cation channels are thought to be a putative pathway of Ca^{2+} entry; however, the molecular mechanisms remain unclear. We have previously demonstrated that lysophosphatidic acid (LPA), a bioactive phospholipid present in human plasma, sensitizes the response of $[Ca^{2+}]_i$ to mechanical stress in cultured smooth muscle cells, cultured lung epithelial cells, and cultured lens epithelial cells. Using real-time confocal microscopy, local increases in $[Ca^{2+}]_i$ in several regions within the cell subjected to mechanical stress were clearly visualized in cultured bovine lens epithelial cells and cultured vascular endothelial cells in the presence of LPA. We called the phenomenon "Ca^{2+} spots". Pharmacological studies revealed that the Ca^{2+} spot is an elementary Ca^{2+}-influx event through MS channels. In this review, possible physiological and pathophysiological roles of LPA as a mechanosensitizer are discussed.
Keywords: lysophosphatidic acid; mechanotransduction; mechanosensitive ion channel; intracellular Ca^{2+} ion concentration

イメージングで解き明かす生命機能

第8回　細胞傷害機構のイメージング

川西　徹，河合　洋 Toru Kawanishi/Hiroshi Kawai（国立医薬品食品衛生研究所）
E-mail：kawanish@nihs.go.jp／URL：http://www.nihs.go.jp/

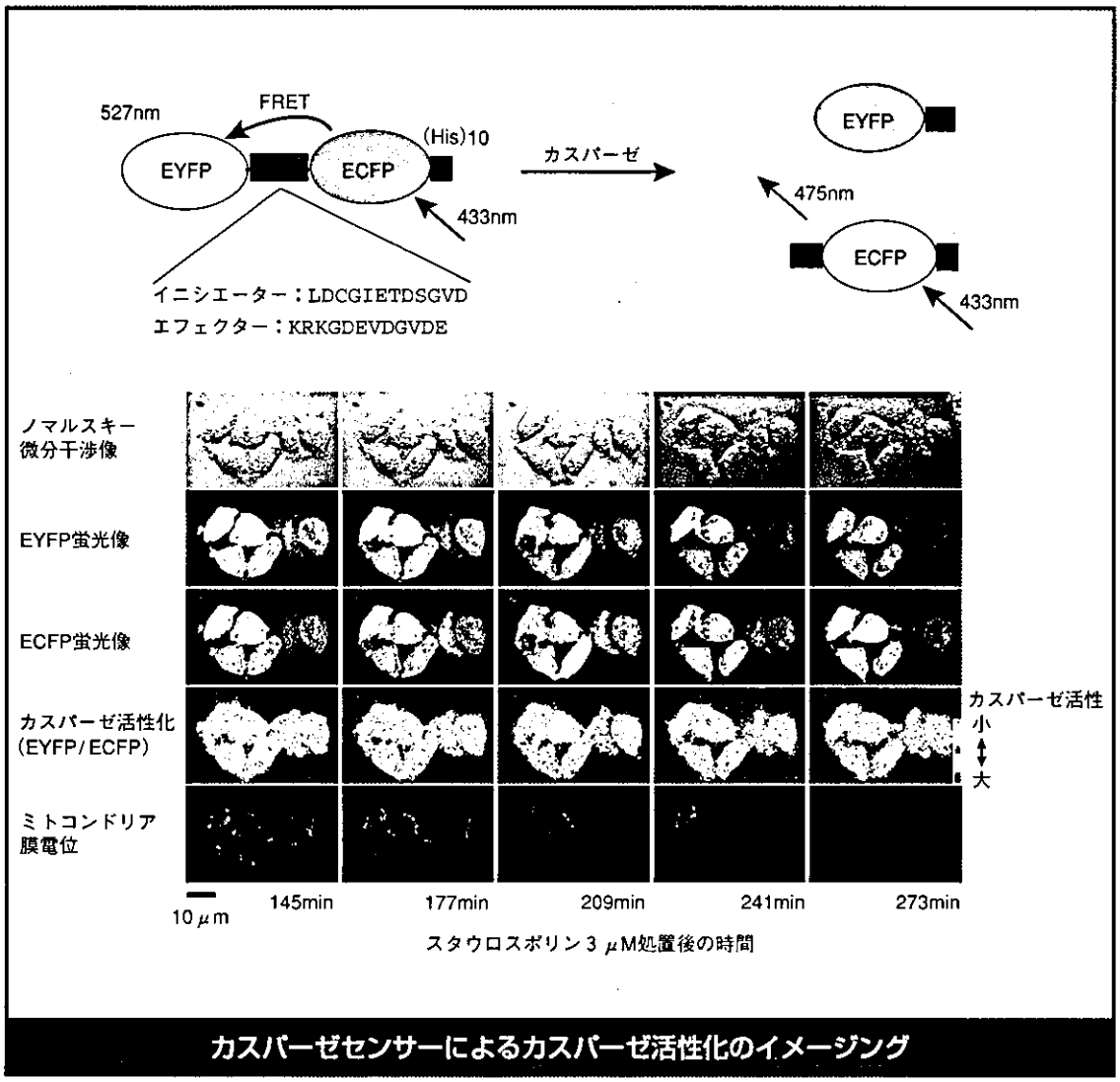

カスパーゼセンサーによるカスパーゼ活性化のイメージング

カスパーゼセンサーとして，イニシエーターカスパーゼおよびエフェクターカスパーゼによって特異的に切断されるペプチド鎖（それぞれLDCGIETDSGVDおよびKRKGDEVDGVDE）の両端にECFPとEYFPを融合した蛍光性タンパク質をデザインした．この融合タンパク質の発現用プラスミドを作製し，HeLa細胞に遺伝子導入，発現させた．写真はエフェクターセンサーの共焦点レーザー走査顕微鏡像である．カスパーゼの活性化はEYFPの蛍光強度とECFPの蛍光強度との比（EYFP/ECFP）の減少として検出される（写真では擬似カラー表示）．ミトコンドリアの膜電位はテトラメチルローダミンメチルエステルを用いてイメージングしており，蛍光像の消失は脱分極を表す．

背　景

近年，細胞傷害におけるアポトーシスの役割が注目されている．アポトーシスは生理的条件下で細胞自らが積極的に引き起こす細胞死であるが，個体が誕生，成長，さらに生存を続けるうえで必要な基本メカニズムと考えられている．一方，このメカニズムは細胞傷害時にも作動し，種々の疾患の発症にも関係する．このアポトーシス誘導メカニズムにおいては，カスパーゼとよばれる一連のシステインプロテアーゼが細胞内で順次活性化され，このカスケードが細胞死の情報伝達に重要な役割を果たしている．しかしそれぞれのカスケード反応過程が細胞内のどの場所でどのようなタイミングで生じているかは明らかでない．そこで，このカスパーゼ活性化のイメージングを試みた．

カスパーゼの活性化を視る

カスパーゼは哺乳類動物では12種類程度存在することが知られているが，アポトーシス刺激後，イニシエーターカスパーゼ（カスパーゼ8/9など）がまず活性化を受け，これがエフェクターカスパーゼ（カスパーゼ3/6/7など）の特異的ペプチド配列を切断し活性化する．そこで，図に示すような蛍光性タンパク質性プローブ（カスパーゼセンサー）をデザインした．この融合タンパク質は，ペプチド鎖が活性化カスパーゼによって切断されるとECFP→EYFPの蛍光共鳴エネルギー遷移（fluorescence resonance energy transfer：FRET）が減少し，蛍光が変化する．すなわちECFPを励起したときのECFP，EYFPの蛍光を測定し，その蛍光強度比（EYFP/ECFP）像のイメージングにより，カスパーゼ活性化を視ることができると考えられる．カスパーゼセンサーのイメージングは共焦点レーザー走査顕微鏡LSM510システムを用いて行った．励起光は458nm（Arレーザー）を用い，ECFP領域およびEYFP領域の蛍光測定に最適化したフィルター（おのおの467.5～497.5nm，および515～545nm）を用いて画像を得た．

HeLa細胞で発現した融合タンパク質はTNF-αあるいはスタウロスポリンによるアポトーシス刺激によって切断され，イニシエーターセンサーは主としてカスパーゼ8/9によって，エフェクターセンサーはカスパーゼ3によって切断されることを確認した．次にカスパーゼ活性化と同じくアポトーシス誘発メカニズムと密接に関係しているミトコンドリア膜電位変化との同時イメージングを行った．ミトコンドリア膜電位は，膜電位依存的にミトコンドリアに取り込まれるテトラメチルローダミンメチルエステルを用いて，543nm（He/Neレーザー）の励起光，560nm以上の蛍光測定によってイメージングした．その結果，アポトーシス刺激（TNF-α 200ng/ml，スタウロスポリン3μM）後に生じる蛍光変化のタイミングは細胞個々で大きく異なる（1～数時間後）ものの，カスパーゼの活性化は細胞個々についてはミトコンドリア膜電位の脱分極と10分程度以下の時間差で生じることが明らかとなった．イニシエーターカスパーゼ活性化とエフェクターカスパーゼの活性化は，測定蛍光波長が同一であるため，同一細胞での観察は不可能である．しかし細胞個々についてのミトコンドリア膜電位の脱分極との比較を介して活性化のタイミングを比較したところ，平均するとイニシエーターカスパーゼはエフェクターカスパーゼより5～10分程度速く活性化されること，さらにTNF-αはスタウロスポリンより5～10分程度速くこれらのカスパーゼを活性化することが明らかとなった（現在投稿中）．このように，アポトーシス刺激からカスパーゼ活性化まで長時間の経過が必要であるが，カスパーゼ活性化およびミトコンドリア膜電位の脱分極という，アポトーシスメカニズムに重要なカスケード反応は，きわめて短時間のうちに生じることが，画像化によって明らかにされた．

今後の展望

現在，複数のカスパーゼ活性化を異なった蛍光波長で検出し，同一細胞での同時観察を可能にするためのプローブ，あるいはアポトーシスメカニズムにかかわるその他の生化学現象を画像化するためのプローブの開発を継続して行っている．これらのプローブを用いることにより，アポトーシスメカニズムの視覚化が可能となり，細胞傷害メカニズムが詳細に解明され，細胞傷害の治療薬の開発などに利用されるものと思われる．

この研究の一部は厚生労働科学研究費補助金（萌芽的先端医療技術推進研究事業）によった．

● 使用機器 ●

・共焦点レーザー走査蛍光顕微鏡LSM510：カールツァイス　TEL：03-3355-0332／FAX：03-3358-7554
・蛍光フィルター：Chroma Technology Corp.　URL：http://www.chroma.com

J. Biochem. **136**, 81–87 (2004)
DOI: 10.1093/jb/mvh103

Protective Properties of Neoechinulin A against SIN-1–Induced Neuronal Cell Death

Kiyotoshi Maruyama, Takashi Ohuchi, Kenji Yoshida, Yasushi Shibata, Fumio Sugawara and Takao Arai*

Department of Applied Biological Science, Faculty of Science and Technology, Tokyo University of Science, Yamazaki 2641, Noda 278-8510

Received February 24, 2004; accepted April 30, 2004

Peroxynitrite ($ONOO^-$) is thought to be involved in the neurodegenerative process. To screen for neuroprotective compounds against $ONOO^-$-induced cell death, we developed 96-well based assay procedures for measuring surviving cell numbers under oxidative stress caused by 3-(4-morpholinyl) sydnonimine hydrochloride (SIN-1), a generator of $ONOO^-$, and sodium *N,N*-dietyldithiocarbamate trihydrate (DDC), an inhibitor of Cu/Zn superoxide (O_2^-) dismutase. Using these procedures, we obtained a microbial metabolite that rescued primary neuronal cells from SIN-1-induced damage, but not from DDC-induced damage. By NMR analysis, the compound was identified as neoechinulin A, an antioxidant compound that suppresses lipid oxidation. We found that the compound rescues neuronal cells such as primary neuronal cells and differentiated PC12 cells from damage induced by extracellular $ONOO^-$. However, non-neuronal cells, undifferentiated PC12 cells and cells of the fibroblast cell line 3Y1 were not rescued. Neoechinulin A has scavenging, neurotrophic factor-like and anti-apoptotic activities. This compound specifically scavenges $ONOO^-$, but not O_2^- or nitric oxide (NO). Similar to known neuroprotective substances such as nerve growth factor and extracts of *Gingko biloba* leaves, neoechinulin A inhibits the SIN-1-induced activation of caspase-3-like proteases and increases NADH-dehydrogenase activity. These results suggest that neoechinulin A might be useful for protecting against neuronal cell death in neurodegenerative diseases.

Key words: free radical scavengers, neoechinulin A, neuroprotective effect, oxidative stress, peroxynitrite.

Peroxynitrite ($ONOO^-$) is produced from superoxide (O_2^-) and nitric oxide (NO) (*1*). O_2^- is highly toxic to neurons as it initiates the chain-reactive production of various reactive oxygen species (ROS) during metabolism; protection against O_2^--induced toxicity is critical for neuronal survival (*2*, *3*). NO has diverse physiological functions (*4–7*) and is toxic to neuronal cells (*8*). NO reacts with O_2^- in a diffusion-limited manner to form the more toxic oxidant $ONOO^-$ (*1*), which induces the death of PC12 cells (*9–11*) and cortical neurons (*12*). In the central nervous system, $ONOO^-$ can be generated by microglial cells activated by pro-inflammatory cytokines or β-amyloid peptide and by neurons (*13*). $ONOO^-$ is far more selective than other strong oxidant and preferentially reacts with thiols (*14*). In addition, $ONOO^-$ also reacts with tyrosine to yield 3-nitrotyrosine (*15*). Increasing levels of nitrotyrosine (*16*) are associated with degenerating neurons in the Alzheimer's disease brain, suggesting pathogenic roles for $ONOO^-$.

SIN-1 (3-(4-morpholinyl) sydnonimine hydrochloride) is a vasodilator that spontaneously releases O_2^- and NO into the medium, thereby producing $ONOO^-$ (*17*, *18*). The compound causes a concentration-dependent increase in cortical cell injury (*19*). It has been reported that neurotrophic factors such as nerve growth factor (NGF) (*20*), and free radical scavengers such as uric acid (*21*) and manganese (III) tetrakis (4-carboxyphenyl) porphyrin (Mn-TBAP) (*22*), rescue neuronal cells from SIN-1-induced damage. However, these compounds prevent oxidative damage caused by various ROS as well as $ONOO^-$-induced damage.

Copper/zinc superoxide dismutase (Cu/Zn-SOD) is highly expressed in neurons (*23*). Thus, an SOD-inhibitor, sodium *N,N*-dietyldithiocarbamate trihydrate (DDC) elevates the amounts of intracellular O_2^- and induces oxidative damage through the chelathor of Cu^{2+} in the active site of Cu/Zn-SOD (*24*, *25*). To obtain compounds that specifically protect neuronal cells against $ONOO^-$-induced oxidative damage, we screened microbial metabolites that rescue primary neuronal cells from SIN-1-induced injury, but not from DDC-induced injury. We obtained a microbial metabolite that specifically protects against $ONOO^-$-induced cell death. In this paper, we describe the neuroprotective properties of this compound.

MATERIALS AND METHODS

Culture of Fungi and Extraction of Their Metabolite—Fungi were isolated as described by Inoue *et al.* (*26*) and incubated at room temperature for 21 d. Each culture was filtered through cheesecloth to remove the mycelia, and the components were extracted with CH_2Cl_2. The

*To whom correspondence should be addressed. Tel: +81-4-7122-9387, Fax: +81-4-7123-9767, E-mail: takarai@rs.noda.tus.ac.jp

